Coherent interference induced transparency in self-coupled optical waveguide-based resonators

Linjie Zhou,* Tong Ye, and Jianping Chen

State Key Laboratory of Advanced Optical Communication Systems and Networks, Department of Electronic Engineering, Shanghai Jiao Tong University, Shanghai 200240, China

**Corresponding author: ljzhou@sjtu.edu.cn*

Received September 21, 2010; revised November 17, 2010; accepted November 18, 2010; posted November 29, 2010 (Doc. ID 135503); published December 16, 2010

We propose a self-coupled optical waveguide (SCOW)-based resonator to generate an optical resonance analogous to electromagnetically induced transparency (EIT). The EIT-like effect is formed by the coherent interference between two resonance paths inherent to the SCOW resonator. For cascaded SCOW resonators, the spectrum they produce is significantly affected by the phase shift between them, with the EIT-like peak flattened or split as the two extreme cases. We also investigate the dispersion characteristics of an infinite array of SCOW resonators and show that the dispersion relation and group index in the EIT subband can be greatly changed by a small phase shift between the SCOW resonators.

OCIS codes: 130.3120, 230.5750, 230.4555.

Electromagnetically induced transparency (EIT) has attracted much research interest in recent years, owing to its agility in optical signal buffering, biochemical sensing, and quantum signal processing. EIT was originally observed in atomic vapors [1], and yet the narrowness of the EIT window and the complexity of constructing atomic vapor systems restrict the practical use of the EIT effect. To make better use of the EIT effect, classic all-optical analogies are realized on various platforms, including coupled resonance systems [2–5], photonic crystal waveguides and microcavities [6], plasmonic nanostructures, and metamaterials [7,8].

The on-chip realization of EIT-like effects using microring resonators marks a step forward for coherent manipulation of optical signals for delay, storage, and nonlinear and quantum information processing on a compact integrated platform with room temperature operation. An EIT-like resonance spectrum can be generated in coupled resonators with various configurations, among which series- and parallel-coupled microring resonators are the most widely investigated structures. In series-coupled optical resonators, the EIT-like effect is generated because of the mode splitting and classic destructive interference between two resonators [2,3]. In parallel-coupled optical resonators, the EIT-like effect is generated because of destructive interference between two frequency-detuned resonators through side-coupled parallel bus waveguides [4,5]. Because the resonances for coherent interference come from separate resonators, the resonance frequencies need to be precisely controlled to within their resonance linewidth; as a result, there are stringent design and fabrication requirements for such schemes.

In this Letter, we propose a self-coupled optical waveguide (SCOW)-based resonator to generate an EIT-like spectrum with an interference mechanism different from that of conventional coupled-resonator systems. The uniqueness of our structure is that it relies on two inherent resonance paths provided by a single SCOW resonator to produce the desired destructive interference. It eliminates the need for two separate optical resonators as used in conventional coupled-resonator structures.

Figure 1 shows the schematic of our proposed resonance structure, which is a single bent waveguide self-coupled to form two directional couplers at the input and output ends. Because of self-coupling, light travels back and forth between the two couplers to form a resonance. There are two degenerate resonance modes in the SCOW resonator, one circulating clockwise (CW mode) and the other circulating counterclockwise (CCW mode). The two resonance modes are coupled through the central "bridge" waveguide. Unlike mutual coupling in conventional coupled resonators, self-coupling as in the SCOW resonator allows only unidirectional optical energy transfer, which is feasible only from the CW mode to the CCW mode if input is assumed from the left end.

Using the transfer matrix method, we obtain the transfer functions for the transmission and reflection ports as follows:

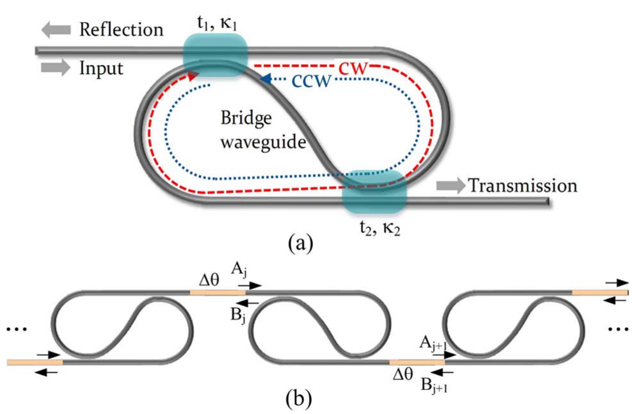

Fig. 1. (Color online) (a) Schematic of a SCOW-based resonator. (b) Schematic of cascaded SCOW resonators. Light circulates in the resonator either clockwise (CW) or counterclockwise (CCW).

$$t_r = -e^{-i\theta}\left[\frac{(\kappa_1 - \kappa_2 e^{-i\phi})(\kappa_2 - \kappa_1 e^{-i\phi})}{(1 - \kappa_1\kappa_2 e^{-i\phi})^2} + \left(\frac{t_1 t_2 e^{-i\phi/2}}{1 - \kappa_1\kappa_2 e^{-i\phi}}\right)^2\right], \quad (1)$$

$$r_r = 2e^{-i\theta}\frac{t_1 t_2 e^{-i\phi/2}}{1 - \kappa_1\kappa_2 e^{-i\phi}}\frac{\kappa_1 - \kappa_2 e^{-i\phi}}{1 - \kappa_1\kappa_2 e^{-i\phi}}, \quad (2)$$

where θ is the phase change associated with the bridge waveguide; t_i and κ_i $(i = 1, 2)$ are, respectively, the transmission and cross-coupling coefficients of the two couplers $(t_i^2 + \kappa_i^2 = 1$ for lossless coupling); and ϕ is the resonator round-trip phase. Resonator loss can be incorporated by replacing $e^{-i\phi}$ with $ae^{-i\phi}$, where a $(a < 1)$ is the loss factor. Resonance occurs at $\phi = 2m\pi$ (m is an integer).

Disregarding the bridge waveguide transmission term $e^{-i\theta}$, the transfer function for the transmission port essentially consists of two terms, representing two coherent resonance paths. The first resonance path stems from light side-coupling with the CW and CCW modes; the second stems from light tunneling through these two resonance modes. These two resonance paths interfere at the transmission output and produce nontrivial resonance features. Figure 2 shows the normalized transmission intensity and phase responses for various combinations of input and output couplers. When their coupling coefficients are close, a narrow transparency peak emerges in the middle of a broad resonance valley, analogous to an EIT spectrum. Phase changes rapidly near the central peak, giving rise to a large group delay. It should be noted that the resonance valley always has two zeros at the transparency window edges owing to the destructive interference, which causes the EIT-like resonance peak to have a high extinction ratio. The transparency window width is determined by the coupling strength. The stronger the coupling is, the narrower the transparency window becomes. In the lossless case, as long as the couplers are identical, the transparency peak is always 1, implying that all the light is transmitted through on resonance. On the other hand, when the coupling coefficients are mismatched and satisfy $|\kappa_1 - \kappa_2| = t_1 t_2$, the resonance profile becomes a deep single valley with its minimum at 0, implying that all the light is reflected back on resonance.

The SCOW resonators can be sequentially connected to form high-order resonance structures, as illustrated in Fig. 1(b). The reflection transfer function, Eq. (2), shows that light can be partially reflected back by the SCOW resonator, and hence Fabry–Perot (FP) resonances can be generated between two adjacent SCOW resonators. The FP resonances can couple with and consequently tailor the EIT-like resonance line shapes.

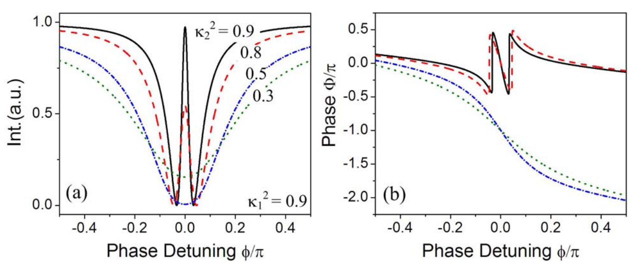

Fig. 2. (Color online) (a) Normalized transmission intensity and (b) phase responses of the SCOW resonator. Loss factor $a = 0.999$.

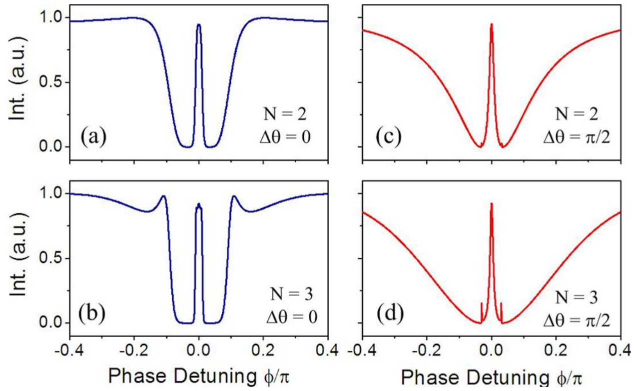

Fig. 3. (Color online) Transmission spectra for cascaded SCOW resonators. Power coupling ratio $\kappa_1^2 = \kappa_2^2 = 0.9$, loss factor $a = 0.999$. N, number of SCOW resonators.

We assume the SCOW resonator circumference, bridge, and connection waveguide lengths are $6L$, L, and $2L$ (L is a unit length), respectively. In the case of no phase shift $(\Delta\theta = 0)$ in the connection waveguides, the FP resonance occurs at $\phi = (2m + 1)\pi$, indicating that the FP and SCOW resonances are totally out of phase and there is minimum coupling between them. Figures 3(a) and 3(b) show the transmission spectra for such cases, with the number of cascaded SCOW resonators $N = 2$ and $N = 3$, respectively. Because there is minimum feedback from the next stage SCOW resonator, the EIT-like resonance spectra do not change significantly except that the transparency window becomes wider at the top and sharper at the edges. On the other hand, when we introduce a $\Delta\theta = \pi/2$ phase shift in the connection waveguide, the FP resonance occurs exactly at the same frequency as that of the SCOW resonator. The in-phase coupling between the FP and SCOW resonances leads to a more significant change of the output resonance profile, as shown in Figs. 3(c) and 3(d). While the resonance valley expands sideward and becomes broader, the central EIT-like resonance peak becomes sharper. Small EIT spikes also emerge alongside the major EIT peak, resulting from the mode splitting induced by mutual resonance coupling, as in conventional coupled resonators. The total number of EIT peaks is equal to $2N - 1$. Note that the side EIT peaks are very narrow and sharp, extremely sensitive to the waveguide loss. With 1 dB/cm waveguide loss incorporated, the side EIT peaks are strongly suppressed and almost not noticeable for the $N = 2$ case.

We also consider an infinite array of lossless SCOW resonators to derive the dispersion characteristics of the SCOW resonances. Based on Bloch's theorem, the electric fields at periodic intervals in the infinite lattice are related by a phase factor, and hence we have (with the same geometric parameters as the previous case)

$$\begin{bmatrix} A_{j+1} \\ B_{j+1} \end{bmatrix} = \frac{1}{t_r t_c}\begin{bmatrix} (t_r^2 - r_r^2)t_c^2 & r_r t_c^2 \\ -r_r & 1 \end{bmatrix}\begin{bmatrix} A_j \\ B_j \end{bmatrix} = e^{-ik_{\mathrm{eff}}L_\Lambda}\begin{bmatrix} A_j \\ B_j \end{bmatrix}, \quad (3)$$

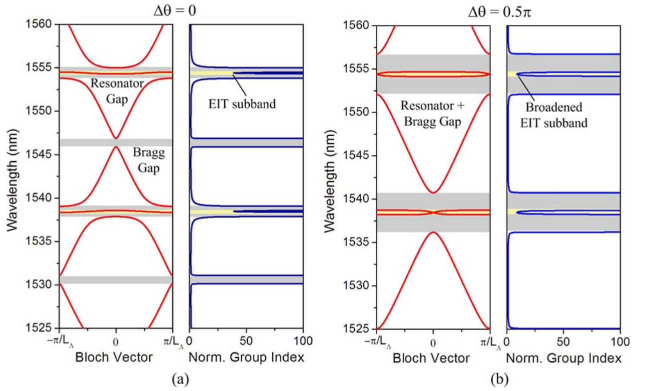

Fig. 4. (Color online) Dispersion diagram and normalized group index of an infinite array of SCOW resonators for two phase shift cases: (a) $\Delta\theta = 0$, (b) $\Delta\theta = \pi/2$.

where $t_c = e^{-i(2\theta+\Delta\theta)}$ is the electric field transmission through the connection waveguide, $\theta = (\phi - \pi)/6$ is determined by the structure parameters, k_{eff} is the Bloch wave effective propagation constant, and $L_\Lambda = 3L$ is the spatial periodicity.

We numerically solve Eq. (3) to get the dispersion relation. Figure 4 shows the dispersion diagram and normalized group index for two phase shift cases. We choose $L = 10\,\mu$m in the calculation. The EIT-like resonances from the SCOW resonators form a narrow subband (EIT subband) inside a broader resonance bandgap in the dispersion diagram. The dispersion curve is relatively flat in the EIT subband, corresponding to a very large group index. The FP resonances that build up between SCOW resonators can also form a Bragg bandgap in the dispersion diagram. At $\Delta\theta = 0$, the two types of bandgaps are equally interleaved and equally far apart, and thus there is the least significant interaction between them. When $\Delta\theta$ is increased to $\pi/2$, the Bragg bandgap overlaps the SCOW resonator bandgap, and, as a result, the dispersion curve in the EIT subband is less flat, leading to a smaller group index and a wider subband width.

The Bragg gap shift therefore provides us a means to tune the slow-light EIT-like modes. As seems intuitive, the tuning is most effective when these two bandgaps are in close proximity. Figure 5(a) shows the minimum normalized group index in the EIT subband and the subband width change as a function of $\Delta\theta$. Figure 5(b) shows the response of the EIT subband to a phase change, $\Delta\theta$, close to $\pi/2$. When the Bragg gap approaches the SCOW resonator gap, the SCOW resonator gap is gradually "pushed" to the other side, and yet the EIT subband is almost fixed around the SCOW resonance wavelength. When $\Delta\theta$ exceeds 0.48π, the two bandgaps overlap and a new EIT subband emerges beside the

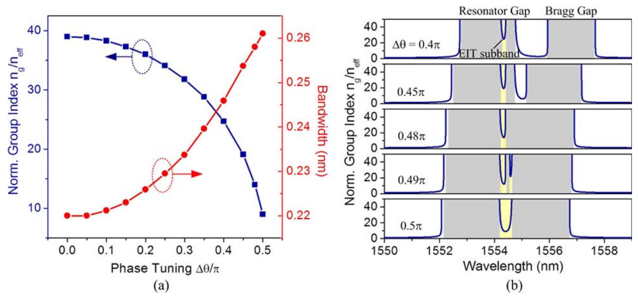

Fig. 5. (Color online) (a) Minimum normalized group index in the EIT subband and its bandwidth change as a function of phase shift $\Delta\theta$ in the connection waveguides. (b) Band diagrams for $\Delta\theta$'s close to 0.5π.

original one, owing to the coherent interference between the two bandgaps. These two EIT subbands finally merge into one when $\Delta\theta = \pi/2$.

In conclusion, we propose a resonance structure, composed of a single bent and self-coupled optical waveguide, to generate an EIT-like resonance. The EIT-like resonances in the cascaded SCOW resonators and the associated narrow transparency subband can be tailored by a phase shift between the SCOW resonators. Given its simple structure and large group index variation, the SCOW resonator and its array can find potential applications in reconfigurable delay lines and nonlinear signal processing.

This work was supported in part by the 973 Program (2011CB301700), the National Natural Science Foundation of China (NSFC) (61007039 and 61001074), the Science and Technology Commission of Shanghai Municipality (STCSM) Project (10DJ1400402), and the State Key Lab Projects (GKZD030020).

References

1. K. J. Boller, A. Imamolu, and S. E. Harris, Phys. Rev. Lett. **66**, 2593 (1991).
2. A. Naweed, G. Farca, S. I. Shopova, and A. T. Rosenberger, Phys. Rev. A **71**, 43804 (2005).
3. D. D. Smith, H. Chang, K. A. Fuller, A. T. Rosenberger, and R. W. Boyd, Phys. Rev. A **69**, 63804 (2004).
4. Y. F. Xiao, X. B. Zou, W. Jiang, Y. L. Chen, and G. C. Guo, Phys. Rev. A **75**, 63833 (2007).
5. Q. Xu, S. Sandhu, M. L. Povinelli, J. Shakya, S. Fan, and M. Lipson, Phys. Rev. Lett. **96**, 123901 (2006).
6. J. Pan, Y. Huo, S. Sandhu, N. Stuhrmann, M. L. Povinelli, J. S. Harris, M. M. Fejer, and S. Fan, Appl. Phys. Lett. **97**, 101102 (2010).
7. N. Liu, L. Langguth, T. Weiss, J. K. Stel, M. Fleischhauer, T. Pfau, and H. Giessen, Nat. Mater. **8**, 758 (2009).
8. N. Papasimakis, V. A. Fedotov, N. I. Zheludev, and S. L. Prosvirnin, Phys. Rev. Lett. **101**, 253903 (2008).